Solar Energy
And Sustainable Development
Refereed, biannual scientific journal issued by
Center for Solar Energy Research and Studies

Validation of Thermal Models for Polycrystalline Photovoltaic Module Under Derna City Climate Conditions

Mahmood Abdel hadi[1], Yasser Aldali[2*], and Ali N. Celik[3]

[1] The Libyan Academy – Benghazi – Libya,

[2]Omar Al Mokhtar University, Faculty of Engineering, Dept. of Mechanical Engineering, Derna – Libya

[3]Abant Izzet Baysal University, Faculty of Engineering and Architecture, Dept. of Mechanical Engineering, Gölköy Campus 14280 Bolu, Turkey.

e-mail: [1]Engmah1982@gmail.com, [2] yasser.aldali@omu.edu.ly [3] celikan@ibu.edu.tr

Abstract: The main objective of the present paper is to compare nine different cell temperature models available in the literature with data measured under real Derna city climatic conditions (a semi arid climate) for month of August. The study focuses on a comparison of nine theoretical models to calculate the cell temperature based on the experimental measurements such as the ambient temperature, irradiance, and wind speed in some of the models. The presently used models are explicit, depending on the easily measurable parameters and of wide applicability. Six statistical quantitative indicators are used to evaluate the cell temperature models analysed, namely, R^2, RMSE, RRMSE, MAE, MBE and MARE. The cell temperature correlations presently studied, first order linear models depending on the ambient temperature, solar irradiation incident on the panel and voltage output, provide the most accurate cell temperature estimations at Derna city climatic conditions

* *Corresponding author*

التحقق من النماذج الحرارية للوح فولتضوئي متعدد التبلر تحت الظروف المناخية لمدينة درنة

محمد عبدالهادى [1]، ياسر الدالى [2] و على سيليك [3]

[1] الاكاديمية الليبية- بنغازي -ليبيا

[2] جامعة عمر المختار- كلية الهندسة- قسم الهندسة الميكانيكية-درنة- ليبيا

[3] جامعة بنت عزة بياسال- كلية الهندسة والعمارة- قسم الهندسة الميكانيكية

قاطع جولكوي- 14280 بوليو تركيا

ملخص: الهدف الرئيسي من هذه الورقة هو مقارنة عدد 9 نماذج لحساب درجة حرارة خلية فولتضوئية متوفرة من دراسات سابقة مع بيانات مقاسه تحت الظروف المناخية لمدينة درنة (مناخ شبه صحراوي) خلال شهر أغسطس . الدراسة تركزت على مقارنة 9 نماذج نظرية لحساب درجة حرارة الخلية بالاعتماد على قياسات تجريبية مثل درجة حرارة المحيط والإشعاع الشمسي وسرعة الرياح في بعض هذه النماذج . تتميز النماذج الحالية بالوضوح وتعتمد على متغيرات سهلة القياس وواسعة التطبيق. استخدمت ستة (6) مؤشرات إحصائية كمية تستخدم لتقييم نماذج درجات الحرارة وهى, R^2 and MBE ,MAE , RRMSE ,RMSE,MARE. العلاقات الرياضية المرتبطة بدرجة حرارة الخلية والتي تم دراستها في هذه الورقة شملت: النماذج الرياضية الخطية من الدرجة الأولى والمعتمدة على درجة حرارة المحيط ، والإشعاع الشمسي الساقط على اللوح و جهد الخرج. كلاهما أعطى نتائج دقيقة عند الظروف المناخية لمدينة درنة.

Keywords: *Photovoltaic, Cell Temperature, Semi Arid Climate, Libya-Derna City.*

1. INTRODUCTION

There are many factors affecting the performance of a PV module. Amongst these some are meteorological variables such as the incident solar radiation on the module, ambient temperature, module temperature, and wind speed. In the past few decades, with the increasing use of PV systems, several studies were carried out on the impact of meteorological parameters such as temperature, radiation, wind speed etc on the performance of PV systems [1,2]. Rehman and El-Amin studied the effect of module temperature on the performance of the polycrystalline modules and showed mathematically the extent of the dependency of the energy efficiency on the module temperature[3]. Ubertini and Desideri investigated the effect of module temperature on the performance of a 15 kW polycrystalline system installed on a rooftop [4]. The study showed that the efficiency decreased by approximately 0.025% for every 1°C increase in module temperature. In Refs. [5,6] the authors reported that the performance of PV systems is a highly location dependent where the climate and the nature of the installation field affect it relatively significant.

Parretta et al reported that 7% of all energetic losses in PV systems are due to a cell temperature effect [7]. They reported that at an ambient temperature of 25°C PV modules will be operating at temperatures above ambient temperatures They can lose up to 14% of their energy production. According to Nishioka et al [8], the temperature coefficient dependence of the system performance was analyzed in order to estimate the annual output of the system in an actual operating environment. As a result, it was found that the annual output energy of their PV system increased by about 1% for an improvement of 0.1%/°C in the temperature coefficient. The authors in Ref. [9] analysed the influence of varying ambient temperatures on the PV panel temperature and validated models for the prediction of cell temperature based on the measured solar radiation and ambient temperature. Pantic et al evaluated and developed linear and nonlinear models to predict the effect of cell temperature on the output power and efficiency of PV modules using five different models for comparison purpose[10]. The results indicated that the nonlinear model provides the most accurate prediction for the temperature of the PV module.

In Refs. [11-20], the researchers developed various thermal models for PV systems taking into account the wind effect on PV cell/module/array temperature calculations. Amongst these research works, Koehl et al. reported a wind cooling effect of 15-20°C for wind speeds of 10 m/s at a solar irradiance of about 1000 W/m² [19].

In this paper, the main objective is to compare nine different cell temperature models available in the literature with data measured in Derna city. In this regard, the article focuses on the comparison of nine theoretical models to calculate the cell temperature based on the experimental measurements of the ambient temperature, irradiance, and wind speed in some of the models.

1.2. Climate in Derna

Derna is a city in the eastern coast of Libya. In Derna, the monthly average daily irradiation on horizontal surface is 5.27 kWh/m² [21]. The mean monthly values of daily irradiation, temperature, wind speed and relative humidity are illustrated in Figure 1. The maximum average wind speed is 4.8 m/s in February and the minimum value is 3.7 m/s in October. The average maximum temperature in Derna is 26.9 °C in August, while the minimum is 14.4 °C in February. As shown in Figure 1, the relative humidity in April is 54.4% whereas it is 60.9% in July.

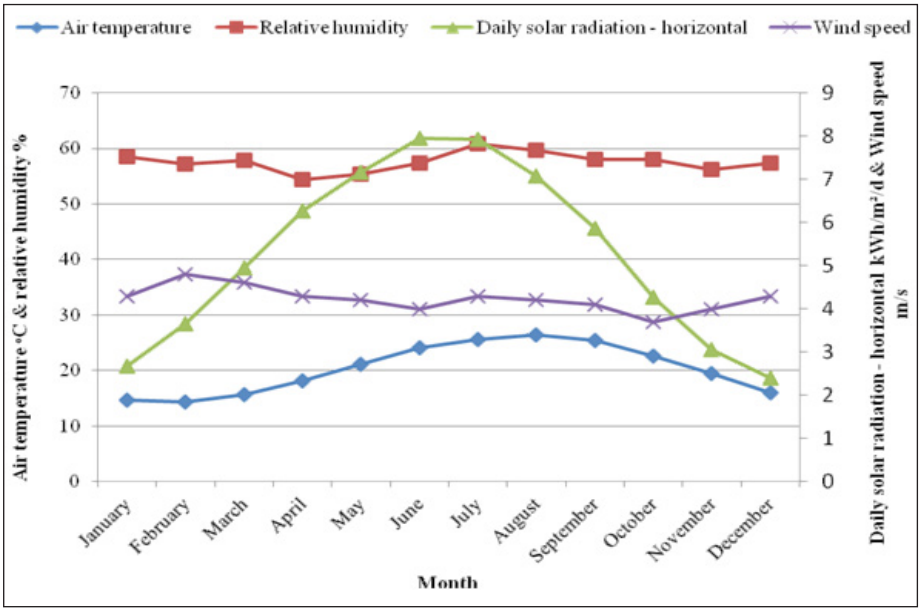

Figure (1). Monthly average ambient temperature, relative humidity, daily solar radiation and wind speed for Derna.

2. EXPERIMENTAL SETUP AND METHODOLOGY

The experimental system consists of a polycrystalline type of PV module with 300 WP of nominal power, situated at the top of a building in Derna (32.75 N; 22.63 E), on the eastern coast of Libya. The module is mounted tilted at an angle equal to the latitude (32.7°) of the location, facing due south. Table 1 shows the technical characteristics of the photovoltaic module.

Table (1). Specifications of the PV module presently used

Electrical specification	
PV model	DS72300
Rated power (Pmax)	300 W
Maximum power voltage (V_{pm})	36.5 V
Maximum power current (I_{pm})	8.22 A
Open-circuit voltage (V_{oc})	45.3 V
Short-circuit current (I_{sc})	8.94 A
Temperature coefficient for maximum power (P_{max})	0.44%/°C
Temperature coefficient for open-circuit voltage (V_{oc})	-0.329V /°C
Temperature coefficient for short-circuit current (I_{sc})	0.038A/°C
Cell efficiency	19.7%
Mechanical specification	
Module area	1.93 m^2
Weight	26.7 kg
Dimensions LxWxH	1955x 880 x 990 mm
Operating conditions	
Ambient operating temperature	-20 °C to 46 °C
NOCT	47.5°C

The data presented in Table 1 are provided by the manufacturer for Standard Test Conditions (STC) of 1000 W/m^2 of irradiance level, 25°C of cell temperature, and 1.5 of air mass (AM 1.5). The PV module under study is made up of 72 cells connected in series, each of 0.024 m^2. Figure 2 shows the photovoltaic module mounted on the roof of a building in Derna, Libya.

Figure (2). Photovoltaic modules mounted at an angle of 32.7° are situated on the top of a building in Derna, Libya

The layout of the experimental system is presented in Figure 3.

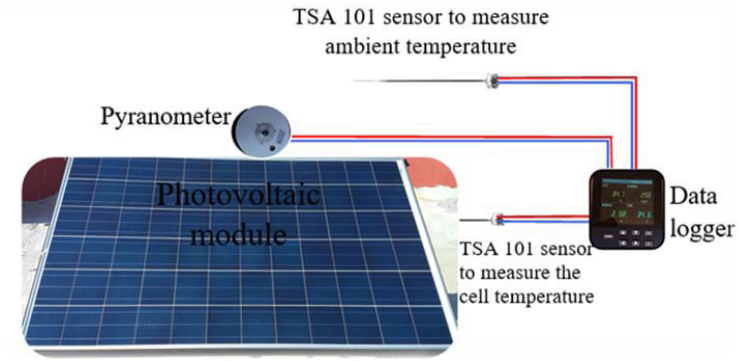

Figure (3). The layout of the experimental setup

For the purpose of measuring cell temperature and meteorological variables, the logging interval is set at a one-minute interval using a 3-channel data logger with RS232 & RS485 connector. One temperature sensor (TSA 101 sensor) is installed and fixed on the back surface of the PV module by thermal tape to measure the cell temperature, and another TSA 101 sensor is installed to monitor the ambient temperature. The measurement of solar radiation data is performed with a RK200-03 pyranometer fixed beside the PV module at the same tilt angle as the PV panel. The measurement range for the pyranometer was 0–2000 W/m^2 over the spectral range of 300–3200 nm.

From the literature, a total of nine cell temperature models are chosen to be used in the present study. These models are chosen because they are commonly used in the literature, dependent on easily measurable parameters and widely applicable. The selected models are presented in Table 2. Five days' worth of PV cell temperature data, collected at the experimental site described above, are used for validating the cell temperature models presently investigated.

Table (2). Photovoltaic cell temperature models used in the present study.

Correlation	Eq.	Comment	Ref.
$T_{cell} = 0.943T_a + 0.0195G_T - 1.528V + 0.3529$	(1)	Linear temperature prediction model	[19]
$T_{cell} = T_a + \frac{G_T}{800}(T_{NOCT} - 20)$	(2)	NOCT used in this study is 47.5 °C	[12]
$T_{cell} = 30 + 0.0195(G_T - 300) - 1.14(T_a - 25)$	(3)	Lasnier 1, for p-Si	[24]
$T_{cell} = T_{ref} + C_1(G_T - G_{200}) - C_2(T_a - T_{a.NOCT})$	(4)	C_1= 0.0175and C_2 = 1.14 was found by Lasnier	[25]
$T_{cell} = T_a + \frac{G_T(T_{NOCT} - 20)}{800}\left[1 - \frac{\eta_{STC}}{\tau\alpha}\right]\frac{9.5}{5.7 + 3.8V}$	(5)	NOCT Dyn 1, use the correlation 1 of McAdams for convection, uses $(\tau\alpha) = 0.81$	[12]
$T_{cell} = T_a + \frac{G_T(T_{NOCT} - 20)}{800}\left[1 - \frac{\eta_{STC}}{\tau\alpha}\right]\frac{8.5}{5.7 + 2.8V}$	(6)	NOCT Dyn 2, use the correlation 1 of Skoplaki for the convection	[13]

$T_{cell} = T_a + \frac{[1 - \eta_{PVSyst}](\tau\alpha) G_T}{U_{LO} + U_{L1V}}$	(7)	PVSyst, $\eta_{PVSyst} = 0.1$, $U_{Lo} = 29 W/m^2/^oC$ and $U_{L1} = 0\ \ W_s/m^3/^oC$	[20]
$T_{cell} = T_a + k_{\Delta T} G_T$	(8)	Skoplaki 2, With $k_{\Delta T} = 0.02 - 0.04\ K.m^2/W$	[26]
$T_{cell} = T_a + \frac{S}{U_{LO} + U_{L1V}}$	(9)	Faiman, use $S = (\tau\alpha) G_T$, $U_{L0} = 30.02 W/m^2/^oC$ and $U_{L1} = 6.28\ Ws/m^3/^oC$	[18]

In Table 2, T_{NOCT} is the so-called nominal operating cell temperature, which is defined as the temperature of the cell at the conditions of the nominal terrestrial environment, I_{NOCT}= 800 W/m², $T_{a,NOCT}$ = 20°C, T_{ref} is the reference temperature, Ta is the ambient temperature , V is the wind speed, GT is the intensity of the solar irradiance, G_{200}=200 W/m² and η_{STC} is the module efficiency at STC .

In the related literature, the goodness of different cell temperature models is assessed based on some typical statistical parameters. In the present study, six of such statistical quantitative indicators are used to evaluate the predictive capability of different cell temperature models presently investigated. The quantitative indicators currently used are given as follows:

1. The root mean squared error (RMSE) is also called the root mean square deviation, (RMSD). The RMSE is a frequently used parameter to compare forecasting errors of different models [27]. The lower the RMSE value is, the better the predictive capability of a model in terms of its absolute deviation is. However, presence of some large errors can result in greater values of RMSE. The RMSE is given by,

$$RMSE = \sqrt{\frac{\sum_{i=1}^{n} (X_{m,i} - X_{c,i})^2}{n}} \quad \text{..... (10)}$$

where $X_{m,i}$ is the measured value, Xc,i is the calculated value of cell temperature and n is the total number of observations.

2. The relative root mean square error (RRMSE) is given by,

$$RRMSE = \sqrt{\frac{\frac{1}{n}\sum_{i=1}^{n} (X_{m,i} - X_{c,i})^2}{\sum_{i=1}^{n} X_{m,i}}} \times 100 \quad \text{..... (11)}$$

This indicator is calculated by dividing RMSE by the average value of measured data. According to [28], model accuracy is considered excellent when RRMSE > 10%, good if 10% < RRMSE < 20%, fair if 20%< RRMSE < 30%, and poor if RRMSE >30%.

3. The mean absolute error (MAE) is the sum of absolute values of the errors divided by the number of observations. This quantity is often used in statistics to measure how close the calculated values are to the measured values. In [27], the authors pointed out some advantages of MAE over the root mean squared error (RMSE) in dimensioned evaluations and inter-comparisons of average model performance error. It is given by,

$$MAE = \frac{1}{n}\sum_{i=1}^{n} |X_{m,i} - X_{c,i}| \quad \text{..... (12)}$$

4. The mean bias error (MBE) [27] is an indicator that expresses a tendency of a model to underestimate (negative value) or overestimate (positive value) a calculated value, while the MBE values closest to zero are

desirable. The drawback of this test is that it does not show the correct performance when the model presents overestimated and underestimated values at the same time, since overestimation and underestimation values cancel each other. The mean bias error is given by,

$$MBE = \frac{1}{n}\sum_{i=1}^{n}(X_{m,i} - X_{c,i}) \quad \text{..... (13)}$$

5- The mean absolute relative error (MARE). is an indicator that is expressed as average absolute value of relative differences between estimated and measured cell temperature values and is given by,

$$MBE = \frac{1}{n}\sum_{i=1}^{n}\left|\frac{X_{m,i} - X_{c,i}}{X_{m,i}}\right| \quad \text{..... (14)}$$

The MARE, when expressed in percentages, is also known as mean absolute percentage error (MAPE) [28].

6- The coefficient of determination (R2) [29] is often used in statistics for estimating the performance of models. It depicts the fraction of the calculated values that are closest to the line of measurement data. While the ideal values of all other statistical indicators used in this study is 0, values of the coefficient of determination close to the unity indicate more efficient models. The coefficient of determination is given by,

$$R^2 = 1 - \frac{\sum_{i=1}^{n}(X_{m,i} - X_{C,i})^2}{\sum_{i=1}^{n}(X_{m,i} - X_{m,avg})^2} \quad \text{..... (15)}$$

$X_{m,avg}$ is the average of the measured data.

3. RESULTS AND DISCUSSION

3.1. Cell Temperature Analysis

The cell temperature of a PV module depends mainly on solar irradiance level incident on the module as well as the ambient temperature. Figure 6 shows the variation of hourly average ambient temperature, cell temperature and the solar irradiance for a particular day in August (2017), measured at the experimental system in Derna city. As seen from the figure, the cell temperature rises from the level of ambient temperature at sunrise to the maximum, which is well above the ambient temperature at around the noon.

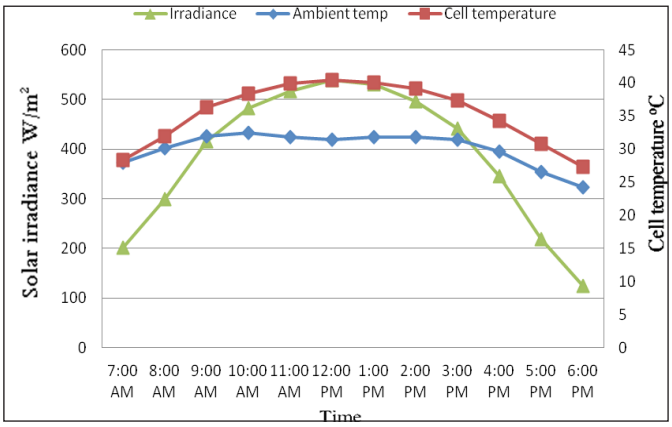

Figure (4). The variation of hourly average ambient temperature, cell temperature and the solar irradiance for a particular day measured at the experimental system in Derna city

As mentioned before, a total of nine cell temperature correlations are being investigated, using five days' worth of PV cell temperature data collected at the experimental site for validation purposes. The cell temperature values calculated from the correlations are given in Figures 5-13 versus the measured cell temperature values.

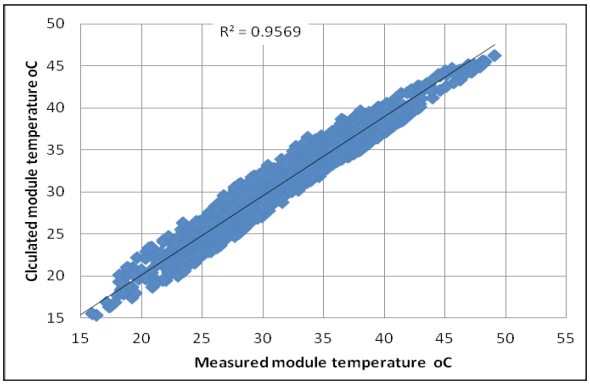

Figure (5). The cell temperature calculated by Eq. (1) versus the measured temperatures.

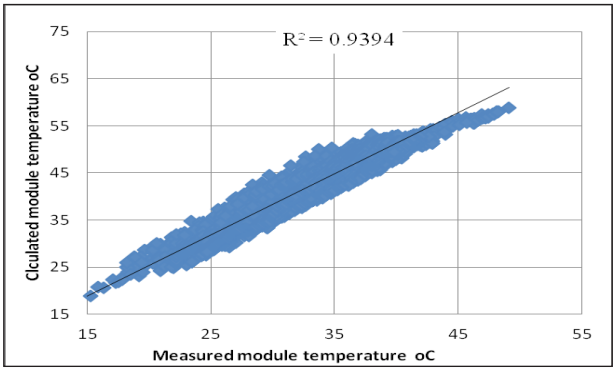

Figure (6). The cell temperature calculated by Eq. (2) versus the measured temperatures.

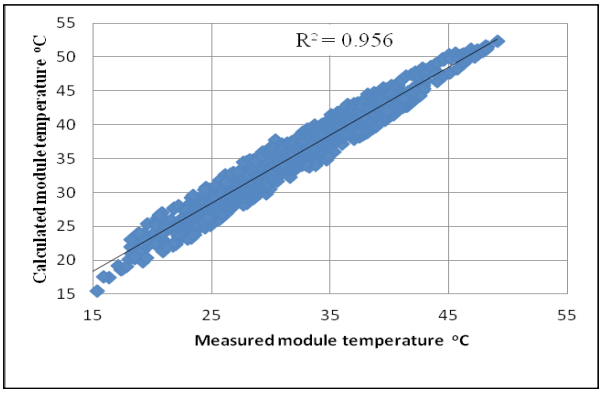

Figure (7). The cell temperature calculated by Eq. (3) versus the measured temperatures.

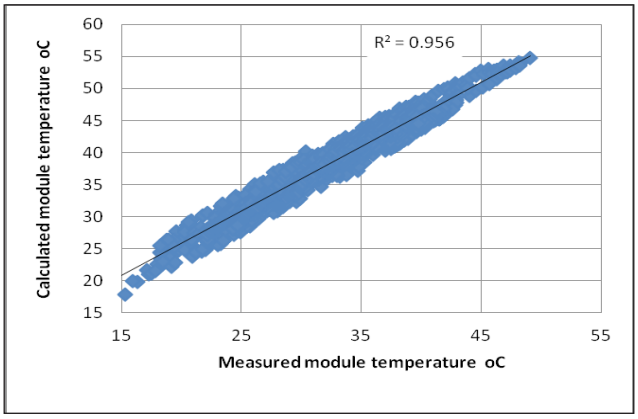

Figure (8). The cell temperature calculated by Eq. (4) versus the measured temperatures.

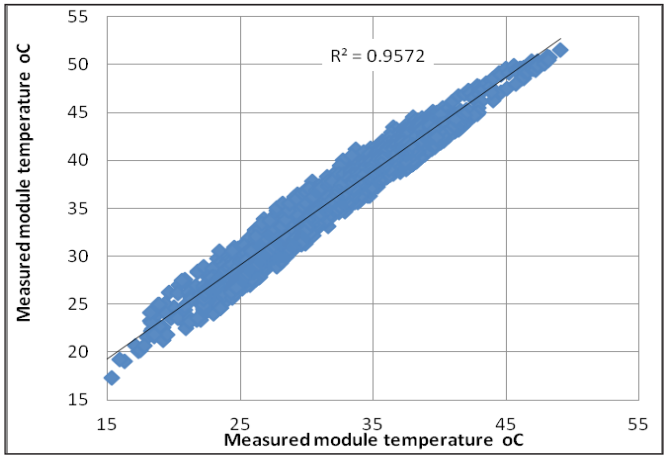

Figure (9). The cell temperature calculated by Eq. (5) versus the measured temperatures.

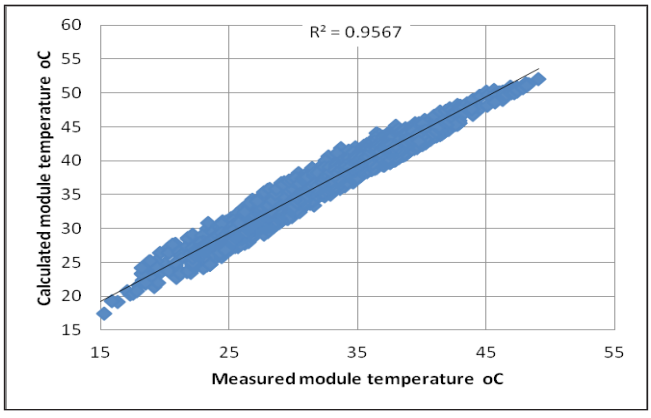

Figure (10). The cell temperature calculated by Eq. (6) versus the measured temperatures.

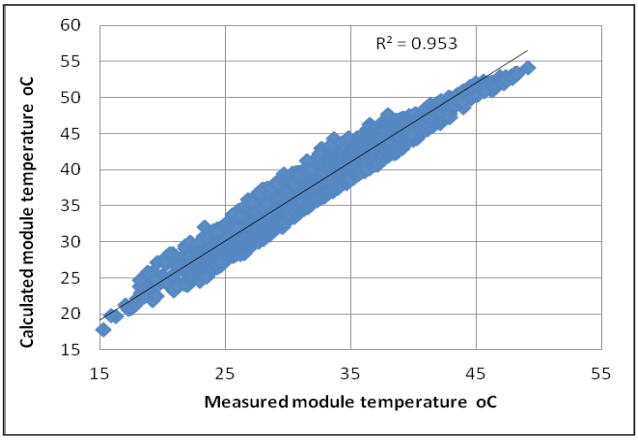

Figure (11). The cell temperature calculated by Eq. (7) versus the measured temperatures.

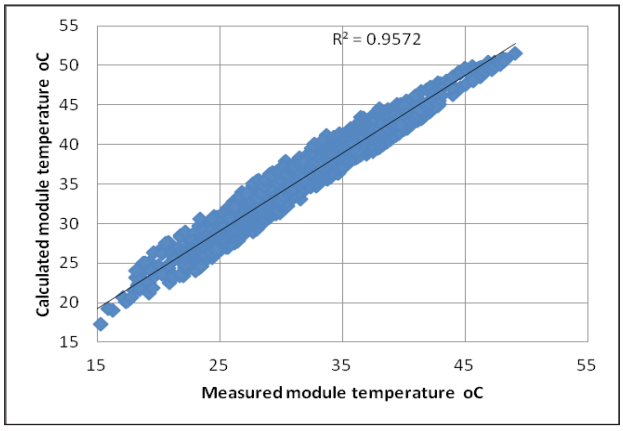

Figure (12). The cell temperature calculated by Eq. (8) versus the measured temperatures.

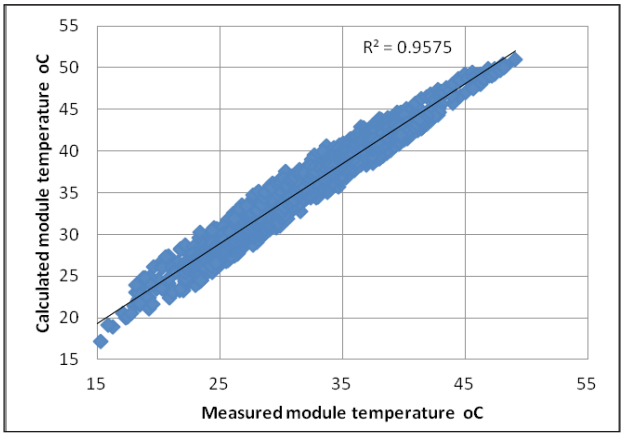

Figure (13). The cell temperature calculated by Eq. (9) versus the measured temperatures.

The statistical parameters presently employed (RMSE, RRMSE, MAE, MBE, MARE and R2) are calculated based on the measured and the estimated cell temperature data for the assessment of the goodness of different cell temperature correlations. The statistical parameters are presented in Table 3. Bold values refer to the most accurate model for the particular indicator. Regarding the statistical parameters presently used, with R^2 being the only exception, the lower the value is, the more accurate the estimate is. As can be seen from Table 3, the models given by Eqs. 1,3,4,5,6,8 and 9 all return the same R^2 values. On the other hand, the models given by Eqs. 2 and 7 return R^2 values of 0.94 and 0.95, respectively. From the table, however, it is interesting to note that the cell temperature correlation given by Eq. 1 provides the most favorable statistical values for the parameters RMSE, RRMSE, MAE, MBE and MARE. It could be safely concluded that the model given by Eq. 1 is by far the most accurate correlation for modeling the cell temperature as far as the presently used data is involved for the city of Derna in Libya.

Table (3). The statistical parameters calculated based on the measured and the estimated cell temperature data

Correlation (Table 2)	RMSE	RRMSE	MAE	MBE	MARE	R^2
1	1.35	0.4	1.00	0.63	0.03	0.96
2	9.79	2.9	9.44	-9.44	0.28	0.94
3	3.67	1.0	3.46	-3.45	0.11	0.96
4	6.03	1.8	5.90	-5.90	0.18	0.96
5	4.47	1.3	4.30	-4.29	0.13	0.96
6	4.51	1.3	4.34	-4.34	0.13	0.96
7	6.08	1.8	5.89	-5.89	0.18	0.95
8	4.14	1.2	3.96	-3.96	0.12	0.96
9	3.76	1.1	3.57	-3.57	0.11	0.96

4. CONCLUSION

The main objective of the present paper is to compare nine different cell temperature models available in the literature with data measured under real Derna city climate conditions for a month of August. Six statistical quantitative indicators (R^2, RMSE, RRMSE, MAE, MBE and MARE) were used to evaluate the goodness of the cell temperature correlations presently studied. Regarding the statistical indicators, the results show that the correlation given by Eq. (1) provided the most accurate cell temperature estimations for the climatic conditions presently analysed.

5. ACKNOWLEDGMENTS

The authors would like to thank Omar Al Mokhtar University, Faculty of Engineering -Derna, for providing all necessary facilities.

6. NOMENCLATURES

Glossary of Symbols & Abbreviations

τ_{α}	Effective transmittance
η_{STC}	The module efficiency at STC
G_{stc}	Solar radiation for standard test conditions W/m2
G_T	Incident solar irradiation Wh/m^2
I_{sc}	Short circuit current of PV module A.
P_{max}	The maximum power under standard test conditions W
$_{Ta}$	Ambient temperature ^oC
Tc	Cell temperature ^oC
T_{ref}	Reference temperature ^oC
V	Volt V
V_{mpp}	Module's voltage at maximum power V.
V_{oc}	Open circuit voltage of PV module V.
X_{ci}	Calculated value of cell temperature.
$X_{m.avg}$	Average of the measured data.
$X_{m.i}$	Measure value.

Abbreviations

AC	Alternating Current.
AM	Air Mass.
DC	Direct Current.
MAE	Mean Absolute Error.
MBE	Mean Bias Error.
MARE	Mean Absolute Relative Error.
NOCT	Nominal Operating Cell Temperature.
PRMSE	Relative Root Mean Square Error
PV	Photovoltaic.
R^2	Coefficient of Determination.
RMSE	Root Mean Square Error.
STC	Standard Test Conditions.

7. REFERENCES

[1]. Carr, A. J., & Pryor, T. L. (2004). A comparison of the performance of different PV module types in temperate climates. Solar Energy, 76(1-3), 285-294.

[2]. Akhmad, K., Kitamura, A., Yamamoto, F., Okamoto, H., Takakura, H., & Hamakawa, Y. (1997). Outdoor performance of amorphous silicon and polycrystalline silicon PV modules. Solar Energy Materials and Solar Cells, 46(3), 209-218..

[3]. Rehman, S., & El-Amin, I. (2012). Performance evaluation of an off-grid photovoltaic system in Saudi Arabia. Energy,

46(1), 451-458.

[4]. Ubertini, S., & Desideri, U. (2003). Performance estimation and experimental measurements of a photovoltaic roof. Renewable energy, 28(12), 1833-1850..

[5]. Khatib, T., Mohamed, A., & Sopian, K. (2013). A review of photovoltaic systems size optimization techniques. Renewable and Sustainable Energy Reviews, 22, 454-465.

[6]. Khatib, T., Sopian, K., & Kazem, H. A. (2013). Actual performance and characteristic of a grid connected photovoltaic power system in the tropics: A short term evaluation. Energy Conversion and Management, 71, 115-119..

[7]. Parretta, A., Sarno, A., & Vicari, L. R. (1998). Effects of solar irradiation conditions on the outdoor performance of photovoltaic modules. Optics Communications, 153(1-3), 153-163.

[8]. Nishioka, K., Hatayama, T., Uraoka, Y., Fuyuki, T., Hagihara, R., & Watanabe, M. (2003). Field-test analysis of PV system output characteristics focusing on module temperature. Solar Energy Materials and Solar Cells, 75(3-4), 665-671.

[9]. Ceylan, İ., Erkaymaz, O., Gedik, E., & Gürel, A. E. (2014). The prediction of photovoltaic module temperature with artificial neural networks. Case Studies in Thermal Engineering, 3, 11-20.

[10]. Pantic, L. S., Pavlović, T. M., Milosavljević, D. D., Radonjic, I. S., Radovic, M. K., & Sazhko, G. (2016). The assessment of different models to predict solar module temperature, output power and efficiency for Nis, Serbia. Energy, 109, 38-48.

[11]. King, D. L., Boyson, W. E., & Kratochvil, J. A. (2004). Photovoltaic array performance model, Sandia National Laboratories, paper nr. SAND2004-3844.

[12]. Duffie, J. A., & Beckman, W. A. (2013). Solar engineering of thermal processes. John Wiley & Sons.

[13]. Skoplaki, E., Boudouvis, A. G., & Palyvos, J. A. (2008). A simple correlation for the operating temperature of photovoltaic modules of arbitrary mounting. Solar Energy Materials and Solar Cells, 92(11), 1393-1402.

[14]. Koehl, M., Heck, M., Wiesmeier, S., & Wirth, J. (2011). Modeling of the nominal operating cell temperature based on outdoor weathering. Solar Energy Materials and Solar Cells, 95(7), 1638-1646..

[15]. Kurtz, S., Whitfield, K., TamizhMani, G., Koehl, M., Miller, D., Joyce, J., & Zgonena, T. (2011). Evaluation of high-temperature exposure of photovoltaic modules. Progress in photovoltaics: Research and applications, 19(8), 954-965..

[16]. Mattei, M., Notton, G., Cristofari, C., Muselli, M., & Poggi, P. (2006). Calculation of the polycrystalline PV module temperature using a simple method of energy balance. Renewable energy, 31(4), 553-567.

[17]. Barroso, J. S., Barth, N., Correia, J. P. M., Ahzi, S., & Khaleel, M. A. (2016). A computational analysis of coupled thermal and electrical behavior of PV panels. Solar Energy Materials and Solar Cells, 148, 73-86.

[18]. Faiman, D. (2008). Assessing the outdoor operating temperature of photovoltaic modules. Progress in Photovoltaics: Research and Applications, 16(4), 307-315.

[19]. Kurnik, J., Jankovec, M., & Brecl, K. (2011). Outdoor testing of PV module temperature and performance under different mounting and operational conditions. Solar Energy Materials and Solar Cells, 95(1), 373-376.

[20]. Kaldellis, J. K., Kapsali, M., & Kavadias, K. A. (2014). Temperature and wind speed impact on the efficiency of PV installations. Experience obtained from outdoor measurements in Greece. Renewable Energy, 66, 612-624.

[21]. NASA Surface meteorology and Solar Energy. http://eosweb.larc.nasa.gov/cgi-bin/sse/retscreen.cgi?email=rets@nrcan.gc.ca.

[22]. Muzathik, A. M. (2014). Photovoltaic modules operating temperature estimation using a simple correlation. International Journal of Energy Engineering, 4(4), 151.

[23]. Kalogirou, S.A., (2009). Solar Energy Engineering: Processes and Systems, USA: Elsevier Inc. Available at: http://dx.doi.org/10.1016/B978-0-12-374501-9.00014-5.

[24]. Charalambous, P. G., Maidment, G. G., Kalogirou, S. A., & Yiakoumetti, K. (2007). Photovoltaic thermal (PV/T) collectors: A review. Applied Thermal Engineering, 27(2-3), 275-286.

[25]. Skoplaki, E. P. J. A., & Palyvos, J. A. (2009). Operating temperature of photovoltaic modules: A survey of pertinent correlations. Renewable energy, 34(1), 23-29.

[26]. Willmott, C. J., & Matsuura, K. (2005). Advantages of the mean absolute error (MAE) over the root mean square error

(RMSE) in assessing average model performance. Climate research, 30(1), 79-82.

[27]. Li, M. F., Tang, X. P., Wu, W., & Liu, H. B. (2013). General models for estimating daily global solar radiation for different solar radiation zones in mainland China. Energy conversion and management, 70, 139-148.

[28]. Jiang, Y. (2009). Estimation of monthly mean daily diffuse radiation in China. Applied Energy, 86 (9), 1458-1464.

[29]. Yadav, A. K., & Chandel, S. S. (2014). Solar radiation prediction using Artificial Neural Network techniques: A review. Renewable and Sustainable Energy Reviews, 33, 772-781.